ENERGY PERFORMANCE OF CHILLERS WITH WATER MIST ASSISTED AIR-COOLED CONDENSERS

K.T. Chan[1], J. Yang[1], and F.W. Yu[2]
[1]The Hong Kong Polytechnic University, Hong Kong, China
[2]Hong Kong Community College, Hong Kong, China

ABSTRACT

This paper reports how the coefficient of performance (COP) of air-cooled chillers can be improved by adopting variable condensing setpoint temperature control and using mist evaporation to pre-cool ambient air entering the condensers to trigger a lower condensing temperature. Chiller models without and with water mist system were established, and the former was validated by using measured operating data of an installed screw chiller. With the validated model, the energy performance of air-cooled screw chillers with twin refrigeration circuits and water mist system serving a representative commercial building was studied. The results reveal that the chiller COP can be changed by various degrees from -0.3% up to +72% depending on the weather and load conditions, and the annual energy consumption can be reduced by 10.9% for a commercial building in subtropical climate.

INTRODUCTION

Air-cooled chillers are commonly used to provide cooling in commercial buildings, particularly in densely populated cities in shortage of water, but with considerable electricity consumption (Yik, Burnett et al. 2001). Low operational efficiency especially under partial load conditions and poor control are part of the reasons for such huge energy consumption. The deficient performance of air-cooled chillers is mainly due to head pressure control (HPC). HPC means that the number of staged condenser fans is kept minimal in order to allow the condensing temperature to hover around its high set point of 50^{o}C. The condenser fan power under HPC can be minimized, but the chiller COP decreases considerably when the chiller load drops in moderate outdoor temperatures. Some researchers have stated the opportunity to lower the condensing temperature to save compressor power to improve the operating efficiency of air-cooled chillers (Manske, Reindl et al. 2001). All the condenser fans under variable condensing temperature control (CTC) are staged in most operating conditions. This causes an increase in the fan power, but the condensing temperature can be kept lower to minimize the compressor power and hence to maximize the chiller COP.

Currently, most of the air-cooled chillers are equipped with constant speed condenser fans (CSF). The extent of the condensing temperature decrease is constrained by the dry-bulb temperature of outdoor air. Evaporative cooling can reduce the air temperature from its dry bulb to wet bulb temperature. Therefore, it is possible to improve the energy efficiency of air-cooled chillers by installing water mist system to pre-cool the outdoor air before entering condensers. The water mist pre-cooling system is not a new concept, and has been applied successfully in the industries (Cheung, Santos et al. 2006; Hsieh and Yao 2006; Zhang, Yongfeng et al. 2007). However, the application of water-mist system associated with a chiller system is not common, and a limited number of studies are found on the performance of chillers with water mist system . Yu and Chan (2009) studied the application of water mist by simulation, which indicated that water mist could improve chiller efficiency noticeably. However, these models are developed based on only one refrigeration circuit.

The aim of this paper is to investigate the energy performance of air-cooled chillers with twin refrigeration circuits and the features of variable speed condenser fans, variable condensing temperature control and water mist. A chiller plant serving an air-conditioned office building was considered in order to show the effects of each feature on the annual electricity consumption of chillers.

MODEL DEVELOPMENT

One of the objectives is to investigate the chiller performance under CTC, but there is a lack of such operating data. Currently nearly all the air-cooled chillers operate under HPC, there is no reset of the condensing setpoint temperature at changes of operating conditions, and a detailed simulation of chiller with twin refrigeration circuits is needed.

System and model descriptions

The air-cooled chiller plant installed in an institutional complex was investigated, which comprises of five identical chillers connected in parallel. The chiller had a nominal cooling capacity of 1105 kW, and the rated electric power demand of each chiller was 398 kW. The chiller has two identical refrigeration circuits in parallel and each circuit is equipped with an electronic expansion valve and two screw compressors, which is shown in Figure 1. The air-cooled condenser contains 16 identical condenser fans in eight groups to deliver a total airflow rate of 85.5 m^3/s, and each refrigeration circuit operates with four fan groups. The power of each fan is 2.1 kW and the total fan power is 33.6 kW when all the condenser fans are operating. The chiller operated under head pressure control with constant speed condenser fans, and the operating variables were monitored by a building management system (BMS).

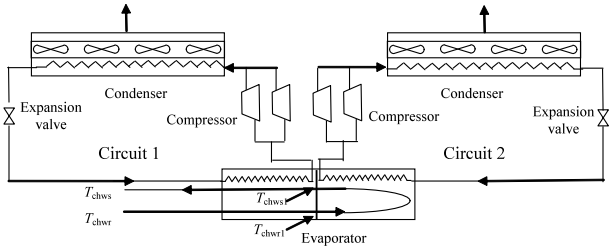

Figure 1 Schematic of the air-cooled screw chiller

Modelling of twin circuit chillers

The chiller model was developed using the Transient Simulation Program TRNSYS, based on the field chiller mentioned before. As this chiller has two identical refrigeration circuits, designated as 1 and 2, the chiller can operate with one refrigeration circuit or both according to changes of cooling load. In this paper, in order to highlight the effect of variable condensing temperature control, the general control strategy calls for one refrigeration circuit when chiller load is less than half of the rated chiller capacity and keeps the load of both circuits equal when the total chiller load is more than half of the rated chiller capacity. The cooling load of the chiller can be expressed by the following equations,

$$Q = m_w \cdot c_w \cdot (T_{chwr} - T_{chws}) \quad (1)$$

$$Q = Q_1 + Q_2 \quad (2)$$

The cooling load of circuit 2 (Q_2):

$$Q_2 = m_w \cdot c_w \cdot (T_{chwr1} - T_{chws1}) \quad (3)$$

The cooling load of circuit 1 (Q_1) is the sum of cooling load of the two sections,

$$Q_1 = Q_{11} + Q_{12} \quad (4)$$

$$Q_{11} = m_w \cdot c_w \cdot (T_{chwr} - T_{chwr1}) \quad (5)$$

$$Q_{12} = m_w \cdot c_w \cdot (T_{chws1} - T_{chws}) \quad (6)$$

Where m_w is the chilled water mass flow rate, C_w is the specific heat capacity of water, T_{chws1} and T_{chwr1} are the chilled water temperature entering and leaving refrigeration circuit 2, respectively.

The condensing setpoint temperature (T_{cd}) influences the heat rejection airflow required for any given cooling capacity and chiller performance. Heat rejection (Q_{cd}) involves the energy and mass balance in the condenser and is calculated by Eq. (7) and Eq. (8). Q_{cd} could be met by modulating heat rejection airflow (V_a) through staging different numbers of condenser fans or changing their speed. To control T_{cd} at its setpoint, V_a has to comply with inequality (9). The lower boundary of the required V_a was given by Inequality (10) which is obtained from Inequality (9). T_{cdsp} was the set point of condensing temperature and was used to determine the staged condenser fans. For any Q_{cd}, the number of staged condenser fans (N_{cf}) was determined by using Inequality (12), which was based on Eq. (11) and Inequality (10).

$$Q_{cd} = Q + E_{cc} \quad (7)$$

$$Q_{cd} = V_a \rho_a C_{pa} (T_{cdal} - T_{cdae}) \quad (8)$$

$$T_{cdal} = \frac{Q_{cd}}{V_a \rho_a C_{pa}} + T_{cdae} < T_{cd} \le T_{cdsp} \quad (9)$$

$$\frac{Q_{cd}}{\rho_a C_{pa} (T_{cdsp} - T_{cdae})} < V_a \quad (10)$$

$$V_a = \frac{V_{a,tot}}{N_{cf,tot}} N_{cf} \quad (11)$$

$$\frac{N_{cf,tot}}{V_{a,tot} \rho_a C_{pa}} \cdot \frac{Q_{cd}}{(T_{cdsp} - T_{cdae})} < N_{cf} \quad (12)$$

To avoid having too much detail here, the other equations for the chiller components can be referred to a previously reported chiller model (Chan and Yu 2006), which are applicable to each refrigeration circuit. The flow chart in Figure 2 excluding the water mist model presents the procedure to

determine the operating variables of the chiller without water mist. The programme starts with the model initialization using the input data. As the chiller load can be shared by the refrigeration circuits randomly, the strategy load sharing should be specified first, then whether only one refrigeration circuit or both circuits will run can be determined. Then, the evaporating temperature and pressure of circuits 1 and 2 (T_{ev1}, T_{ev2}, P_{ev1} and P_{ev2}) and the cooling loads of the three sections of the heat exchangers (Q_{11}, Q_{12} and Q_2) are calculated through an iterative procedure by assuming a value for Q_{11} firstly. Once the model has determined the evaporating temperature and pressure of circuits 1 and 2, the model evaluates the state variables of each refrigeration circuit. As the condensing temperature interacts between the compressor and condenser components, an iterative procedure is implemented to solve the operating variables of the two components simultaneously. The number of staged condenser fans and the corresponding airflow are computed according to a condensing setpoint temperature, which is another iterative loop. The convergence criterion for computing condensing temperature and evaporating temperature in this model is 0.01°C, and the convergence criterion for the cooling load shared by the first section of the heat exchanger in circuit 1 Q_{11} is 0.01 for the relative error. When a converged solution has been obtained by iterations using specified convergence criterion, all the variables of the model can be obtained.

Validation of the chiller model

The validity of the chiller model without water mist was assessed by comparing the modelled results with the measured operating data from a field chiller operating under HPC with constant speed condenser fans, where the outdoor temperature (T_{cdae}) ranges from 24 to 35°C and the part load ratio (PLR) ranges from 0.2 to 1.2.

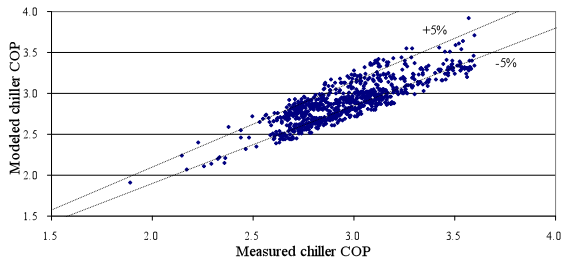

Figure 3 Comparison of modelled and measured chiller COP

Figure 3 shows a comparison of the modelled and the measured chiller COP. There are two lines in the figure that give the boundary of ±5% deviation from the ideal case. For most of the data, the uncertainty (i.e., the difference between the modelled value and the experimental value) of chiller COP is less than 10% and the uncertainty is even less than 5% for more than half of these data. Having this chiller model validated and used as a basis, other advanced control of condensing temperature (e.g. CTC) and alternative condenser designs using VSF and water mist can be modelled and simulated.

VSF model

The potential benefits of using variable speed condenser fans were analysed, considering that they can operate at lower speed with much reduced power while helping improve the controllability of the condensing temperature. With variable speed fans, V_a can be adjusted continuously based on any given setpoint of condensing temperature. An integrated group of condenser fans running simultaneously at same speed was assumed for each refrigeration circuit. Given that the chiller studied had two refrigeration circuits, the condenser model contained a total of two separate group of variable-speed fans, each of which consumed a rated power of 16.8 kW and provided a rated airflow of 42.76 m^3/s at the full speed of 15.8 rps. It was assumed that the variable-speed drive consumed 3% of the total power of the staged condenser fans at any speeds. Figure 2 shows the procedure for computing the fan number (N_{cf}), rotating speed (R_{cf}) and power (E_{cf}) of the staged condenser fans based on any given V_a .

Applying the fan law, the rotating speed of each staged fan can be determined by Eq. (13), and the total power input to the staged condenser fans (E_{cf}) is given by Eq. (14), where R_{cfr} is the full speed of the fans and $E_{cf,ea}$ is the rated power of one condenser fan. The fan speed is proportional the fan airflow and the fan power is proportional to the third power of fan speed.

$$R_{cf} = R_{cf\,r}\frac{V_a}{N_{cf}V_{ar}} \qquad (13)$$

$$E_{cf} = N_{cf}E_{cf,ea}\left(\frac{V_a}{N_{cf}V_{ar}}\right)^3 \qquad (14)$$

Condensing temperature control

With variable speed condenser fans, the strategy for implementing CTC is to reset the condensing setpoint temperature T_{cdsp} following a rule to calculate the trade-off between the compressor power and condenser fan power, resulting in minimum chiller power for any given cooling load and weather condition. To find the optimum setpoint of the condensing temperature ($T_{cdsp,op}$), a logical argument was included in the algorithm of controlling condenser fans. T_{cdsp} increased in steps of 0.05°C from its lower level of 20°C or (T_{cdae}+3°C), whichever is higher.

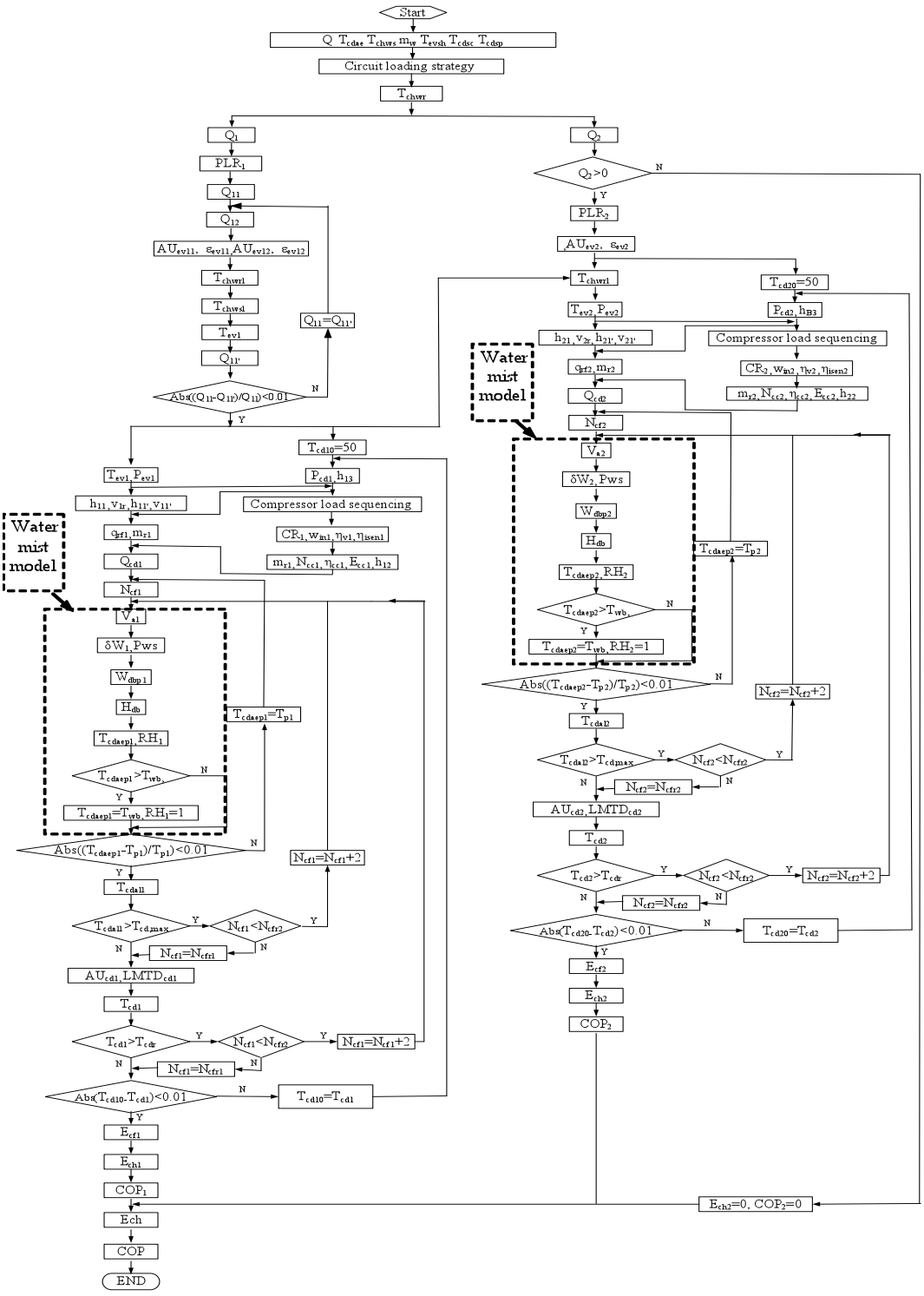

Figure 2 Flow chart of the chiller model

With the change of T_{cdsp}, the chiller power, including compressor and condenser fan power, was calculated and compared with the current minimum value. If the chiller power at the present iteration was smaller than the current minimum value, the minimum chiller power was stored and the corresponding T_{cdsp} was stored as the optimum condensing setpoint temperature. After that, a new iteration started again until T_{cdsp} reached 45°C. For each operating condition, the minimum chiller power along with the optimum T_{cdsp} were able to be identified. Figure 2 presents the procedure to find the $T_{cdsp,op.}$

Water mist model

Figure 4 shows a schematic of a typical water mist system, which comprises of a high pressure pump, filter unit, atomization nozzles, high pressure tubing,

low pressure tubing, etc. The high pressure pump can operate to deliver water through the tubing at a high pressure of around 70 bars, and the water is pumped through atomization nozzles to form a mist of 10 micron sized droplets. When the ultra fine water droplets are sprayed into the atmosphere, they quickly absorb the heat in the environment and evaporate, and then the air temperature entering condensers decreases due to evaporative cooling effect, but the extent of temperature drop is limited by the wet-bulb temperature. The dry bulb temperature *(T_{db})* and relative humidity (RH) of ambient air were monitored to control the two identical water mist installations, each with a high pressure pump rated at 0.75 kW and dedicated to one refrigeration circuit. The water mist systems were designed to provide a total mist generation rate of 0.067 L/s for the studied air-cooled screw chiller.

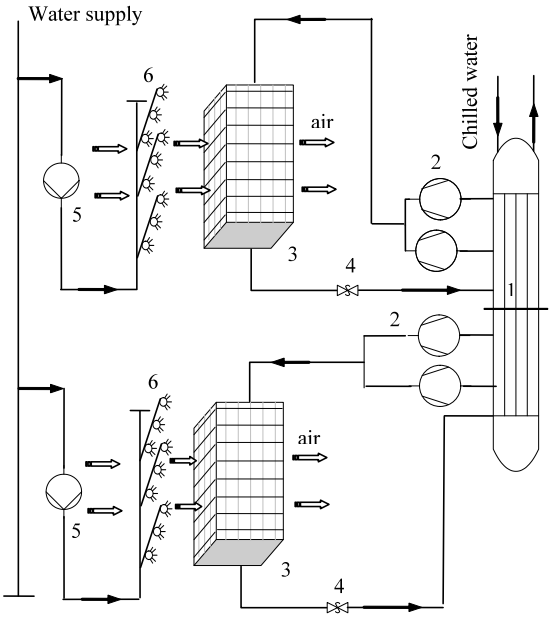

1. Evaporator 2. Compressor 3. Condenser
4.Expansion valve 5.High pressure pump 6. Nozzles

Figure 4 Schematic of the water mist system

At a given temperature and relative humidity of the ambient air, the addition of water vapour in the air due to mist evaporation can be calculated by Eq. (15). The humidity ratio of the ambient air is expressed as Eq. (16), then the humidity ratio of the air at the inlet of condenser can be calculated by Eq. (17).

$$\delta W = m_{mist}/(V_a \rho_a) \quad (15)$$

$$W = 0.622 P_{ws}/(P - P_{ws}) \quad (16)$$

$$W' = W + \delta W \quad (17)$$

In the above equations, δW is the additon of air humidity ratio in unit of kg per kg dry air; P is the total barometric pressure of the moist air in unit of Pa; P_{ws} is the saturation pressure of water vapor in unit of Pa.

The saturation pressure of water vapor in relation to the temperature is given by Eq. (18) (ASHRAE 2009).

$$\ln P_{ws} = C_1/T + C_2 + C_3 T + C_4 T^2 + C_5 T^3 + C_6 \ln T \quad (18)$$

where, T is absolute temperature, K

The specific enthalpy of the moist air in unit of kJ per kg dry air is

$$h = 1.006t + W(2501 + 1.86t) \quad (19)$$

where t is the air dry-bulb temperature, °C.

As the evaporation of water mist is adiabatic and the specific enthalpy of the moist air is constant, the temperature of the air at the condenser inlet can be calculated by Eq. (20).

$$T_{cdae}' = (h - 2501\ W')/(1.006 + 1.86\ W') \quad (20)$$

The relative humidity φ is a function of degree of saturation (μ) as follow.

$$\varphi = \mu/(1 - (1 - \mu) * (P_w / P)) \quad (21)$$

where P_w is the partial pressure of water vapor in the air stream at the given temperature T_{cdae}'.

Degree of saturation μ is the ratio of air humidity ratio W to humidity ratio W_s of saturated moist air at the same temperature and pressure:

$$\mu = W / W_s\big|_{t,p} \quad (22)$$

$$W = \frac{(2501 - 2.326 T_{wb}) * T_{wb} - 1.006 * (T_{cdae} - T_{wb})}{2501 + 1.86 * T_{cdae} - 4.186 * T_{wb}} \quad (23)$$

Before calculating the relative humidity φ of the air at the inlet of the condenser coil, the air humidity ratio W and the saturated air humidity ratio W_s have to be be determined first. The air humidity ratio W at the temperature of the air at the condenser inlet (T_{cdae}') can be calculated by Eq. (23). W_s at the temperature of T_{cdae}' can be calculated using Eqs.(16) and (18) based on the temperature T_{cdae}'.

When the calculated humidity ratio W' is greater than the maximum allowable humidity ratio at the saturation state, or the calculated relative humidity φ is greater than or equal to 1, the air at the inlet of condenser becomes saturation and T_{cdae}' is equal to wet-bulb temperature (T_{wb}). Under such conditions, the water mist generation rate is more than needed, and the surplus water mist droplets would fall down to the ground or be carried to the condenser coil.

From Eq. (15), the amount of water evaporation and change of the humidity ratio is related to the air velocity passing through the condenser coil, hence, the decreased temperature T_{cdae}' at the inlet of condenser is affected by the air velocity. To evaluate the chiller performance, these equations for water mist model are incorporated into the chiller model established before and solved through an iterative prrocedure as shown in Figure 2.

RESULTS AND DISCUSSION

Cooling loads of the office building

In order to assess the energy efficiency of VSF, CTC and water mist system applied to air-cooled chillers with multiple refrigeration circuits in buildings, the cooling energy saving potential for a representative office building in a subtropical climate, as is Hong Kong, was studied. Hourly cooling loads for the representative office building were calculated using EnergyPlus to model the envelope features, building characteristics, lighting, occupancy, ventilation and air conditioning details. The hourly weather data in an example weather year represent the prevailing weather conditions in the local climate.

For the representative office building, the annual cooling energy was 1.00×10^7 kWh and the peak cooling load is 7338 kW. To meet the peak cooling load of 7338 kW, the chiller plant of the office building was designed with seven air-cooled screw chillers, each of which had a nominal cooling capacity of 1105 kW. The size of these chillers is comparable to that of the field-studied chiller report before. The use of equally-sized chillers within a multiple chiller system can facilitate easier implementation of a control strategy and provide more flexible operation and maintenance. The traditional chiller sequencing of a multiple-chiller system is considered in this study, which is to operate the minimum number of evenly loaded chillers to meet the required cooling load.

Improved chiller COP

This study investigates the chiller performance with regard to four cases: HPC+VSF, CTC+VSF, HPC+VSF+WM and CTC+VSF+WM, where WM stands for water mist system. The first one is the base case which is operating under HPC with variable speed condenser fans.

The COP calculation is based on the overall power input to the compressor, condenser fans and high pressure pumps of the mist system. Figure 5 shows the overall chiller COP predicted by the chiller model for a range of PLR without water mist for the base case of HPC+VSF. It shows that the chiller COP varies following the operating sequence of the two refrigerant circuits of the chiller, and the chiller COP drops considerably when one more compressor or refrigeration circuit is staging, because the compressor efficiency drops significantly under low part load ratios. The chiller COP would rise almost linearly with the increasing chiller load when operating certain compressor(s) or refrigeration circuit(s) at any given outdoor temperature, which is different from the fluctuating COP when HPC and constant speed fans were used (Yang et al. 2009).

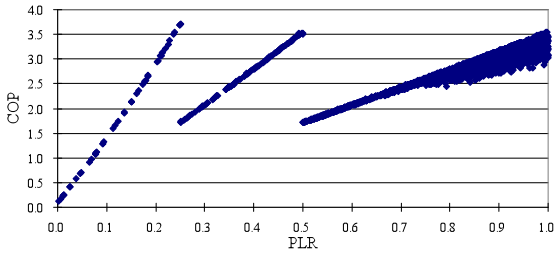

Figure 5 Chiller COP under HPC and VSF

CTC and water mist have different effects on the increase or decrease in the chiller performance. The potential benefits of each condenser feature in relation to the baseline can be identified by the percentage change in chiller COP, as shown in Figure 6 to Figure 8.

After identifying the optimum setpoint of condensing temperature, the improvements in chiller COP can be investigated when the optimum condensing temperature control and variable speed condenser fans are applied to the field-studied air-cooled screw chiller. When CTC and VSF were used together, Figure 6 shows that the chiller COP could increase considerably by up to 71.5% in relation to the base case. The chiller COP under CTC could be improved not only at part load but also at full load. This figure demostrates that the improvement of chiller COP due to CTC varies following the operating sequence of the two refrigerant circuits. The degree of the COP increase is more significant when the chiller PLR is less than 0.5, which means only one refrigeration circuit is activated. When PLR is low, the corresponding outdoor temperatures could be lower as well, and the difference between the condensing setpoint temperature and the outdoor temperature is larger, which reslts in more significant energy saving for the compressors and fans. The improved chiller COP helps reduce the annual electricity consumption of chillers.

When water mist system is applied, the chiller performance could be improved due to the evaporative effect. The temperature difference between dry- bulb and wet-bulb temperature and the relative humidity have great influence on the cooling effect by the water mist system. Figure 7 illustrates that the designed water mist generation rate under

HPC could change the chiller COP by -0.29 to 11.6%. A slight drop in the COP occurred when the relative humidity was more than 95% and the sprayed water mist did not evaporate completely, which had little effect on reducing the entering condenser air temperature. In addition, the high pressure pumps for water mist generation consumed power. When the difference between the dry-bulb and wet-bulb temperature is less than 2°C, the percentage of the chiller COP increased linealy with the temperature difference. However, the relationship between the COP change and the temperature difference did not follow this pattern when the temperature differences were more than 2°C, which was because the installed mist generation rate was less than 50% of the required peak mist genetation rate. It was noted that the installed water consumption rate of 0.067 L/s was small, accounting for only 7.5% of the amount required for a open-loop cooling tower serving a water-cooled chiller with the same cooling capacity, which was 0.89 L/s according to the ARI Standard 550/590 (ASHRAE 2003).

When the chiller operated under CTC with water mist, the energy performance could be further improved. Figure 8 shows that this control strategy brings a considerable increase of 7.1-72.9% in the chiller COP. The extent to which the COP increases tends to be more significant when the chiller load is low with a lower level of relative humidity. At a low chiller load, the difference between the condensing setpoint temperature and the outdoor temperature is larger, and the heat rejection airflow rate can still be high under CTC, which will enable complete evaporation of the generated mist. This, in turn, brings a further decrease in the entering condenser air temperature, which helps reduce the compressor power. Figure 8 illustrates that the percentage change of the chiller COP was almost inversely related to the PLR, and was affected by the change of staged compressors and refrigeration circuits.

Energy saving potential

An analysis was made on how the individual and mixed uses of VSF, CTC and water mist influence the annual electricity consumption of chillers serving the office building. Chilled water pumping energy was not considered here because all the cases studied have the same arrangement of chillers and chilled water pumps.

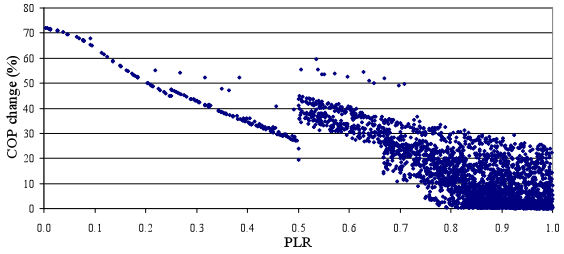

Figure 6 COP improvements by using CTC

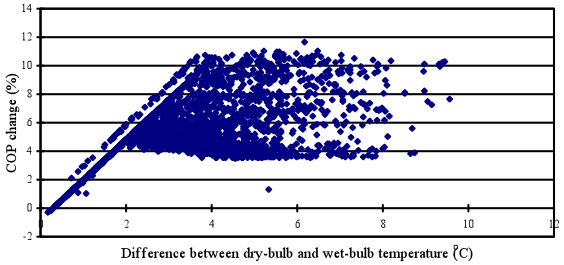

Figure 7 COP improvements by using water mist

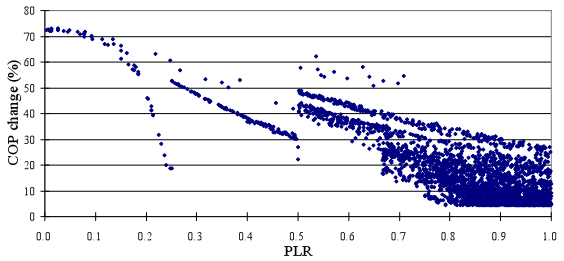

Figure 8 COP improvements by CTC and water mist

According to the building cooling load profile and the schedule of staging chillers, the annual electricity consumption of the chillers and the high pressure pumps was calculated. Table 1 shows the annual electricity consumption of the chiller plant under different operational and control schemes, having variable speed condenser fans in all the cases.

Table 1
Energy performance of chillers using different operational and control schemes

CASE	HPC+VSF	CTC+VSF	HPC+VSF+WM	CTC+VSF+WM
Chiller power consumption (kWh)	3.55×10^6	3.25×10^6	3.33×10^6	3.15×10^6
Saving of chiller power ((%))	-	8.5	6.2	11.3%
High pressure pump consumption (kWh)	0	0	1.57×10^4	1.57×10^4
Annual total power consumption (kWh)	3.55×10^6	3.25×10^6	3.34×10^6	3.16×10^6
Saving of total power consumption (%)	-	8.5	5.8	10.9

When the chillers operated under CTC, the power consumption of the chillers dropped by 8.5% from the baseline. When the chillers operated under HPC with water mist system, the power for the chillers and the high pressure pumps could be saved by 5.8%. When the chiller operated under CTC with water mist, the energy performance was further improved, the total power consumption for operating the chillers and high pressure pumps could drop by 10.9%, and the annual electricity saving was 3.87×10^5 kWh.

CONCLUSION

This paper presents how the individual and mixed condenser features of VSF, CTC and water mist affect the performance of air-cooled chillers. A sophisticated model for an air-cooled screw chiller with variable speed condenser fans and water mist system was developed, and the improved chiller COP with each feature was identified. The year-round cooling load profile of a representative office building in Hong Kong was considered in order to assess how each feature influences the chiller performance and the annual electricity consumption of chillers. The baseline refers to an air-cooled chiller operated under HPC with variable speed fans. The chiller COP could increase by -0.29-12.2% and 3.1-71.9% from the baseline when the chillers operated under the traditional HPC but adding water mist and under the new CTC, respectively. When the chiller operated under CTC with water mist, the energy performance could be further improved, and the chiller COP could increase by 7.1-72.9% from the baseline. It is estimated that the annual electricity savings range from 2.05×10^5 kWh by using water mist to 3.87×10^5 kWh by using CTC together with water mist. Variable speed condenser fans have been used for all these cases. These savings correspond to 5.8-10.9% of the annual electricity consumption of chillers under HPC. This study shows that the energy saving potential in the building sector will be significant by use of VSF, CTC and water mist for air-cooled chillers. The results of the study will prompt low-energy operation of conventional air-cooled chillers working at different weather and load conditions year-round, for cities where scarcity of water resource is a problem. The results reported in this study refer to a subtropical climate, but the energy enhancement is anticipated to be even higher when appling water mist to air-cooled chillers in a dry climate.

ACKNOWLEDGEMENT

The work described in this paper was supported by the central research grant of The Hong Kong Polytechnic University, Project Codes: RP1R and G-U871.

REFERENCES

ASHRAE, Standard 550/590. 2003. Performance rating of water chilling packages using the vapor compression cycle. American Society of Heating. Refrigerating and Air Conditioning Engineers, Arlington, GA.

ASHRAE. 2009. ASHRAE Handbook — Fundamentals, American Society of Heating, Refrigerating and Air-conditioning Engineers, Inc. , Atlanta, GA.

Chan, K. T. and Yu F. W. 2006. Thermodynamic - behaviour model for air-cooled screw chillers with a variable set-point condensing temperature. Applied Energy 83(3): 265-279.

Cheung, N., C. A. Santos, et al. 2006. Application of a heuristic search technique for the improvement of spray zones cooling conditions in continuously cast steel billets. Applied Mathematical Modelling 30(1): 104-115.

Hsieh, C.-C. and Yao S.-C. 2006. Evaporative heat transfer characteristics of a water spray on micro-structured silicon surfaces. International Journal of Heat and Mass Transfer 49(5-6): 962-974.

Manske, K. A., Reindl, D. T. et al. 2001. Evaporative condenser control in industrial refrigeration systems. International Journal of Refrigeration 24(7): 676-691.

Yang, J., Chan, K.T., and Wu X.S. 2009. Optimum operation of air-cooled chillers with multiple refrigeration circuits. Proceedings of 6th international symposium on heating, ventilating and air conditioning. Nanjing, China.

Yik, F. W. Burnett, H., J., et al. 2001. Predicting air-conditioning energy consumption of a group of buildings using different heat rejection methods. Energy and Buildings 33(2): 151-166.

Yu, F. W. and Chan, K. T. 2006. Modelling of the coefficient of performance of an air-cooled screw chiller with variable speed condenser fans. Building and Environment 41(4): 407-417.

Yu, F. W. and Chan, K. T. 2009. Modelling of improved energy performance of air-cooled chillers with mist pre-cooling. International Journal of Thermal Sciences 48(4): 825-836.

Zhang, Yongfeng, Fang Yudong, et al. 2007. Experimental Study of the Interation Between the Water Mists and PVC Fire. Process Safety and Environmental Protection 85(1): 39-44.